

the relation

$$\mathcal{J}^{(2)}/\hbar^2 = \frac{1}{d^2E/dI^2} \approx \frac{4}{[E_\gamma(I+1) - E_\gamma(I-1)]}$$

where $E_\gamma(I) = E(I+1) - E(I-1)$ is the transition energy for the transition, $(I+1) \rightarrow (I-1)$. When comparing with theory, we note that

$$\mathcal{J}^{(2)}/\hbar^2 = \left(\frac{d^2E}{dI^2} \right)^{-1} = \frac{dI}{d\omega} = \sum_{\text{occ}} \frac{d\langle j_x \rangle}{d\omega}$$

where the last equality is valid in the cranking approximation. Furthermore, we have used the canonical relation,

$$\omega = \frac{dE}{dI}$$

to obtain the rotational frequency from the spectrum. Thus, in the cranking approximation, $\mathcal{J}^{(2)}$ is a sum from single-particle terms measuring how the alignment $\langle j_x \rangle$ changes with rotational frequency. It is then instructive to consider how the alignment occurs in a high- j shell, see fig. 12.20 drawn for a $h_{11/2}$ shell at $\varepsilon = 0.25$. The general features of this figure remain for other high- j shells and also for larger deformation. At large deformations, however, the different orbitals get aligned at a higher frequency. As $\mathcal{J}^{(2)}$ measures the increase in alignment, it is evident that the lowest high- j orbital contributes at a very small frequency (fig. 12.20), the next at a somewhat higher frequency and so on.

Realistic calculations illustrating how $\mathcal{J}^{(2)}$ is built for the superdeformed bands in the $A \approx 150$ region are shown in fig. 12.21. Note that, for many particles in a shell, $\mathcal{J}^{(2)}$ is essentially constant similar to what was found in the pure oscillator where no orbital gets a strong alignment. Also, the first, second and third orbitals in a j -shell contribute as anticipated above. The fourth orbital becomes anti-aligned at low frequencies but it gives a positive contribution to $\mathcal{J}^{(2)}$ at higher frequencies. This means that, at superdeformation, high- j shells with four particles or more will contribute with an approximately constant value to the $\mathcal{J}^{(2)}$ moment of inertia.

From the analysis of the observed $\mathcal{J}^{(2)}$ moment of inertia for the superdeformed bands in $^{146}_{64}\text{Gd}_{82}$ – $^{153}_{66}\text{Dy}_{87}$, it has been possible to extract probable configurations for most of these bands (Bengtsson *et al.*, 1988, Nazarewicz *et al.*, 1989). The configurations are specified by the number of particles in high- j (or rather high- N) shells, which according to the discussion above give characteristic contributions to $\mathcal{J}^{(2)}$. A large number of superdeformed bands have also been identified in the Hg/Pb region. These nuclei show a very rich structure as indicated from the plot of calculated bands in fig. 12.22.

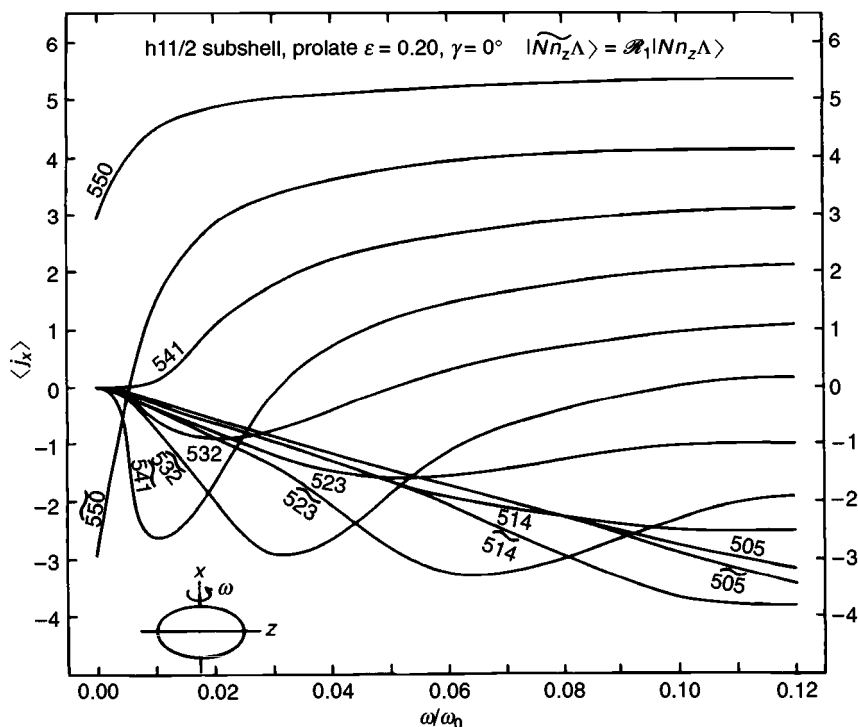


Fig. 12.20. Single-particle angular momentum component along the rotation axis for the $h_{11/2}$ orbitals at prolate shape, $\epsilon = 0.2$. The orbitals are labelled by their asymptotic quantum numbers. The two-fold degeneracy is broken (cf. fig. 12.16) and the two sets of noninteracting orbitals (having different signature), are drawn with and without a 'tilde'. As discussed also in chapter 11, it is the polar orbitals at the bottom of the shell which become strongly aligned. The figure would be very similar for another high- j shell like $i_{13/2}$ or $j_{15/2}$ and it would also be qualitatively unchanged at a larger deformation, however with the alignment becoming more gradual (from Andersson et al., 1976).

Recently, superdeformed rotational bands with identical or almost identical transition energies have been identified in several neighbour nuclei both in the $A = 150$ and in the $A = 190$ regions. This has inspired a lot of experimental as well as theoretical investigations so we will discuss it in some more detail.

12.9 Identical bands at superdeformation

The first identification of almost identical bands in neighbouring nuclei at superdeformation came very much as a surprise. Indeed, as the spins are not known, what is really known with certainty from experiment is that